



# Synthesis, Characterisation, DFT Studies and Electrochemical & Biological Application Studies of A new Schiff base Based on from Naphthalene-1, 8-diamine and Its Co(II), Ni(II), Cu(II) and Zn(II) Complexes

GEETHA THAMARAICHELVAN and SANTI SAMBAMOORTHY\*

PG & Research, Department of Chemistry, Seethalakshmi Ramaswami College, Affiliated to Bharathidasan University, Tiruchirappalli 620 002, Tamil Nadu, India.

\*Corresponding author E-mail: santhi.muthuraman@yahoo.com

<http://dx.doi.org/10.13005/ojc/400631>

(Received: July 22, 2024; Accepted: November 02, 2024)

## ABSTRACT

A new Schiff base 4,4'-((naphthalene-1,8-diylbis(azanylylidene))bis(methanylylidene))diphenol (NDBDP) has been synthesized from 4-hydroxybenzaldehyde and 1,8-diaminonaphthalene and characterised by Infrared, Ultraviolet-Visible, Proton-1 Nuclear Magnetic Resonance, Carbon-13 Nuclear Magnetic Resonance and mass spectral studies. Further, the Schiff base has been complexed with Cobalt(II), Nickel(II), Copper(II) and Zinc(II). All the synthesised complexes are established as neutral complexes based on various spectral, analytical and magnetic behavioral studies. The redox property of all the metal Schiff base complexes have been explored through cyclic voltammetry analysis. Density Functional Theory (DFT) studies have been performed using GAUSSIAN09W program with B3LYP/6-31G (d,p) as the basis set to substantiate the structure of Schiff base NDBDP. The synthesized Schiff base and its transition metal complexes have been scrutinised for their biopotency namely antimicrobial, anti-inflammatory and antioxidant activities. The complex  $[\text{Cu}(\text{NDBDP})_2]$  is found to possess high antioxidant activity. The cytotoxic behaviour of the  $[\text{Cu}(\text{NDBDP})_2]$  complex was scrutinized in MCF-7 (human breast cancer cell lines) which indicate the moderate cytotoxic behaviour of the complex.

**Keywords:** Schiff base, Metal complexes, Anticancer, Antioxidant, Anti-inflammatory.

## INTRODUCTION

Organic reactions involving the condensation of two or more molecules produce novel compounds with high biological behaviors. Schiff bases are significant because of their activity to stabilize metal ions of different oxidation states, broad range of biological spectrum and

their involvement in various industrial and catalytic applications. Because of the presence of a lone pair of electrons on the azomethine group ( $-\text{N}=\text{CH}$ ) Schiff bases form stable complexes with metal ions. Imine complexes possess biological applications such as antimicrobial<sup>1,2</sup>, antiviral<sup>3</sup>, anticancer<sup>4</sup>, antitumor<sup>5</sup>, antioxidant<sup>6</sup> and anti-inflammatory activities<sup>7</sup>. Furthermore, imine complexes are applied



in immobilization of enzymes. The biopotency<sup>8</sup> of Schiff bases is possible because of the presence of azomethine group present in Schiff bases. The simple synthetic routes and the wide applications in numerous areas, including biology, make Schiff bases and their metal complexes find a conspicuous place in research.

With the above facts in mind, in the present study, a new Schiff base was suitably designed and synthesized by the reaction between of 4-hydroxybenzaldehyde and naphthalene -1,8-diamine. The Cobalt(II), Nickel(II), Copper(II) and Zinc(II) complexes of the Schiff base have also been synthesized. The Schiff base was assigned a suitable structure based on various spectral studies. DFT calculations were manipulated to support the assigned structure of the Schiff base. Estimation of metal percentage, thermal analysis, conductance quantification and different spectral recordings (IR, UV-Vis & EPR at LNT) were executed for all the synthesized complexes. Based on the results, suitable structures were assigned to the complexes. The redox properties of all the complexes were also studied to establish the catalytic application. The biological applications like antifungal, antibacterial, antioxidant and anti-inflammatory activities were studied for all the synthesized; compounds, and anticancer activity for the Cu(II) complex was delineated.

## EXPERIMENTAL METHODS

### Spectral and Analytical Studies

The IR spectrum of the compounds was recorded with FT-IR spectrophotometer (model; Spectrum RXI), NMR spectrum with BRUKER AVIII500 and BRUKER AVIII HD and UV-Visible spectra with Perkin Elmer Spectrometer. The mass spectrum of the Schiff base was taken with a Q-T Mass spectrometer in Electro Spray Ionization (ESI). JES; FA200 spectrometer was used for recording the EPR spectrum of the copper complex. TGA/DTA analyses were performed in the temperature ranging from 40 to 730°C. The Elico conductivity bridge was used to determine the molar conductance of all four synthesized complexes in DMSO medium at a concentration of about  $10^{-3}$  M. Standard procedures were adopted for metal estimation studies. The magnetic property was analysed with Gouy Balance. The redox properties of all four complexes were

analysed at room temperature. The electrodes used are glassy electrode, silver-silver chloride electrode and platinum electrodes. During the study, tetrabutylammonium perchlorate was used as a supporting electrolyte.

### Biological activity

#### Antimicrobial activity

The antifungal and antibacterial properties of all the synthesized compounds were analyzed in an agar medium following a good diffusion method. The bacterial pathogens taken for the study were *Staphylococcus aureus* and *Klebsiella pneumoniae* and the fungal pathogens studied were *Candida albicans* and *Aspergillus niger*. The diameter zone of inhibition revealed the bio potency of the compounds.

#### Antioxidant activity

For the study of antioxidant property DPPH scavenger assessment is applied. DPPH is an easily available and stable organic nitrogen radical  $\lambda_{\max}$  of DPPH is 517nm. A change of color from purple to yellow is observed indicating the absorption of hydrogen atom. The absorption at 517nm decreases corresponding to the increase of antioxidant potential. For the execution of analysis, DPPH solution of 0.1mM in methanol is prepared for which 39 mg of DPPH is taken in 100 mL of methanol. This solution is kept at -20°C. Ascorbic acid (1 mg in 1 mL) is used as the standard. Samples of varying strength namely 500, 250, 100, 50 and 10  $\mu\text{g/mL}$  are subjected to analysis. Each time 300  $\mu\text{L}$  of the sample 100  $\mu\text{L}$  of DPPH solution is added, shaken well and kept aside for 30 min under room temperature. Finally, the absorbance was recorded by keeping the  $\lambda_{\max}$  at 517nm. Scavenging effect = %inhibition = [(absorbance of control - absorbance of reaction mixture) / absorbance of control] X 100. Graph Pad Prism 6.0 software (USA) is utilized for calculation of %inhibition and  $\text{IC}_{50}$  value.

#### Anti-inflammatory activity

Inflammation is caused by protein denaturation. Anti-inflammatory activity is nothing but inhibition of the above-mentioned denaturation. For this study, the method developed by Mizushima and Kobayashi and Sakat *et al.*, were followed. Acetyl salicylic acid (Sigma Aldrich) was taken as

the standard. The Schiff base NDBDP was taken at various strength namely 500, 250, 100, 50 and 10 µg/mL. To each test sample 500 µL of 1% bovine serum albumin (Himedia, India) was added. All the test mixtures were heated 20 min at 51°C after keeping at room temperature for 10 minutes. Absorbance was measured at 660nm after the samples cool down to room temperature. The formula adopted for calculation is,

$$\% \text{ Inhibition} = 100 - ((A1 - A2) / A0) * 100$$

A1-absorbance of control, A2-absorbance of test sample and A0-absorbance of positive control.

The analysis was done in triplicate and the results are averaged.

#### Anticancer activity

A 10% FBS, 100 µg/mL of the antibiotic penicillin, and 100 µg/mL of streptomycin were added to liquid DMEM. The above mixture is kept under an atmosphere of CO<sub>2</sub> at 310K. This medium was used for culturing MCF-7 cells bought from NCCS, Pune. With the help of MTT assay, using MCF-7 cells, the *In vitro* cytotoxicity of the copper complex was explored. The cancer cells cultured as above were taken in a tube and harvested by trypsinization. A tissue culture plate in DMEM was saturated with 10% FBS and 1% antibiotic solution for a period of 48 h at 310 K. Sterile PBS was used to wash the wells. Copper complex solutions of different concentrations were then applied in the DMEM medium having no serum. A 5% CO<sub>2</sub> humidified incubator was used for the incubation of cells. The incubation was done for 24 h at 310K. Each well 20 µL of MTT was added at the end of the incubation period.

#### Synthesis of Schiff base NDBDP and its Metal Complexes

Naphthalene-1,8-diamine (0.1 mmol) dissolved in 30 mL of ethanol and 4-hydroxy benzaldehyde (0.2 mmol) in 30 mL ethanol were mixed and stirred for 2 h under room temperature. The dark blue powder deposited was filtered and washed with a pet. ether. DMSO is a suitable solvent for the Schiff base. The melting point is 188°C.

The Schiff base NDBDP (0.2 mmol) and the respective metal chlorides (0.1 mmol) (CoCl<sub>2</sub>, NiCl<sub>2</sub>, CuCl<sub>2</sub> & ZnCl<sub>2</sub>) were refluxed in ethanol at a temperature of 60°C for 3 Hours. The complexes

formed were filtered and dried. DMSO is found to be a suitable solvent for all the complexes. The decomposition of all 257°C for Co complex, 250°C for Ni complex, 238°C for Cu complex and 220°C for Zn complex.

## RESULTS AND DISCUSSION

### Characterization of Schiff base NDBDP and its Metal complexes

#### FT-IR spectra

The presence of phenolic group<sup>9</sup> is specified by the absorption band at 3415.14 cm<sup>-1</sup>. It also shows that the phenolic group is involved in inter-molecular hydrogen bonding. The absorption bands at 1514.42 cm<sup>-1</sup> and 1444.37 cm<sup>-1</sup> corresponding<sup>10</sup> to C=C stretching authenticate the aromatic nature of the compound. The aromatic nature is further substantiated by the peaks ranging from 830.93 cm<sup>-1</sup> to 761.04 cm<sup>-1</sup>. The >C=N group is confirmed by its stretching vibration band appeared<sup>11</sup> at 1647.57 cm<sup>-1</sup>.

The stretching vibration of the >C=N group occurring at 1647.57 cm<sup>-1</sup> in the Schiff base is shifted to 1630.13-1642.88 cm<sup>-1</sup> in their Co(II), Ni(II), Cu(II) & Zn(II) complexes. This suggests the participation of azomethine nitrogen in coordination<sup>12</sup> with the metals Cobalt(II), Nickel(II), Copper(II) and Zinc(II). The above coordination can be further corroborated by the emergence of a new band in the order of 509.84-539.87 cm<sup>-1</sup> in the complexes corresponding to Metal-Nitrogen bond<sup>13</sup>. (Figure S1-S5).

#### <sup>1</sup>H-NMR spectrum

In the Schiff base NDBDP, a multiplet is observed in the range from δ 6.55 ppm- δ 7.90 ppm, recommending the presence of aromatic protons<sup>14</sup> in the Schiff base. The phenolic proton in the para position of the azomethine<sup>15</sup> group appeared at δ 10.49 ppm. (Figure S6).

#### <sup>13</sup>C NMR spectrum

The <sup>13</sup>C spectrum exhibits a band at δ 150.19 ppm, indicates the presence of phenolic<sup>16</sup> carbon. The azomethine<sup>17</sup> carbon is evidenced by the band at δ 163.79 ppm. The aromatic<sup>18</sup> nature of the compound is evidenced by the appearance of bands in the range of δ 115.51 ppm-δ 135.48 ppm. (Figure S7).

#### Mass spectral studies

In the mass spectrum of the Schiff base NDBDP, the peak that appeared at 367.2464 correlates well with the mass 366.44, calculated for

the molecular formula  $C_{24}H_{18}N_2O_2$  proposed<sup>19</sup> to the same. (Figure S8).

### UV-Visible Spectral studies

The UV-Visible spectrum Schiff base NDBDP shows three bands. The bands at 261.30 nm & 279.90 nm are due to the  $\pi \rightarrow \pi^*$  transition of the aromatic ring 20, and that observed at 343 nm corresponds to  $n \rightarrow \pi^*$  transition occurring in the azomethine group<sup>21</sup>.

The UV-Visible spectrum of the Cobalt(II) complex exhibits spin-allowed transition at 424 nm, and the magnetic moment of 4.63 BM supports the octahedral<sup>22</sup> arrangement around the Cobalt(II) ion. In the Nickel(II) complex the band at 413 nm, can be allocated to the  ${}^1A_1 \rightarrow {}^1B_1$  and  ${}^1A_1 \rightarrow {}^1E_1$  transitions<sup>23</sup>, indicating square planar arrangement around Nickel(II) which is in diamagnetic stable<sup>24</sup>. In the Copper(II) complex, a band appears at 797 nm which may be designated to  ${}^2B_{1g} \rightarrow {}^2E_g$ ,  ${}^2B_{1g} \rightarrow {}^2B_{2g}$  and  ${}^2B_{1g} \rightarrow {}^2A_{1g}$  transitions<sup>25</sup>. The magnetic moment of the Copper(II) metal complex is 1.56 BM, indicates the square planar geometry around<sup>26</sup> Copper(II). The Zinc(II) complex indicates a band at 331 nm, which is attributed<sup>27</sup> to L $\rightarrow$ M (charge transfer) transition, confirming the square planar arrangement in the Zinc(II) complex and also its diamagnetic nature<sup>28</sup>. (Figure S9-S13).

### EPR spectrum

The 'g' value calculated from the EPR determines the ground state. The presence of unpaired electron in  $d_{x^2-y^2}$  orbital lead to  ${}^2B_{1g}$  as the ground state for which  $g_{||} > g_{\perp}$ . For the copper complex,  $g_{||}$  is greater than  $g_{\perp}$ , indicating the presence of unpaired electron in  $d_{x^2-y^2}$  orbital<sup>29</sup>, leading to square planar geometry resulting from Jahn-teller effect (Figure 1).

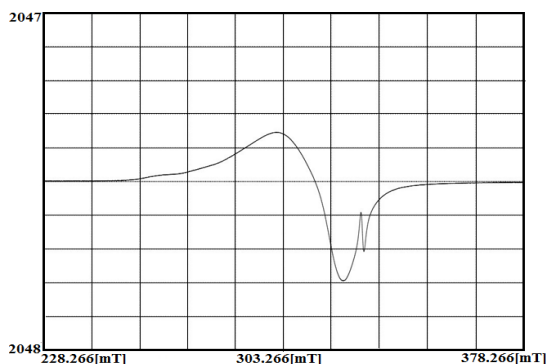


Fig. 1. EPR Spectrum of Copper Complex

### Metal estimation studies

The pyrolytic method is used for cobalt(II) ion estimation. The titrimetric method is followed to determine the quantity of Nickel(II) and Zinc(II) ions, and the Copper(II) ions is ascertained by the colorimetric method. All results comply well with the structures proposed for complexes<sup>30</sup> (Table1).

Table 1: Metal estimation percentage of complexes

Name of the complex	Calculated (P)	Experimental (P)
[Co(NDBDP) <sub>2</sub> ].H <sub>2</sub> O	7.28	7.28
[Ni(NDBDP) <sub>2</sub> ]	7.41	7.3
[Cu(NDBDP) <sub>2</sub> ]	7.98	7.27
[Zn(NDBDP) <sub>2</sub> ]	8.19	8.13

### Conductance measurement

The electrical conductivity of all the synthesized complexes is determined in DMSO medium ( $10^{-3}$  M). Their molar conductance values<sup>31</sup> are found to be present from 17  $\text{ohm}^{-1}\text{cm}^2\text{mol}^{-1}$  to 81  $\text{ohm}^{-1}\text{cm}^2\text{mol}^{-1}$  which authenticates the neutral nature of the complexes.

### Thermal analysis

In the thermal gravimetric analysis of the cobalt complex, the loss of weight occurred between 101°C-194°C (observed 4.42%, calculated 4.35%) and is correlated to the elimination of two molecules<sup>32</sup> of water coordinated to Co(II) ions. The weight loss corresponding to two moles of ligand observed in the range of 194°C-470°C evidences the coordination of two molecules of Schiff base to the Co(II) ions. In the case of the copper complex, the thermal analysis resulted in the first weight loss noticed in the temperature range 105°C-276°C (observed 46.36%, calculated 46.01%) due to the decomposition of one ligand moiety. The second weight loss occurs in the temperature ranging from 277°C-419°C (observed 46.01, calculated 46.50%) corresponds to the disintegration of the ligand moiety<sup>33</sup> confirming the formation of 1:2 metal to ligand complex. After this weight loss, the complex reached constant mass, indicating its dissipation into analog metal oxides. The thermal analysis data are presented in (Fig. 2a & Fig. 2b). The suggested structure of the complexes is presented in Fig. 3a & Figure 3b.

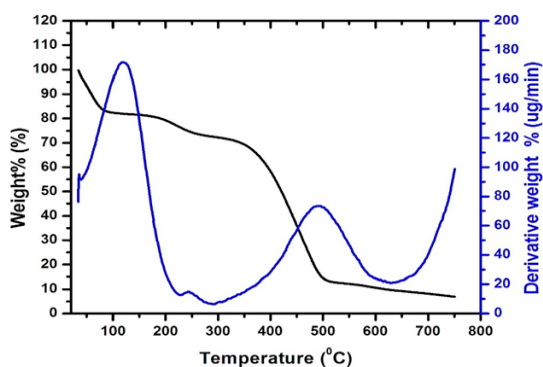


Fig. 2(a). TGA/DTA curve of Co Complex

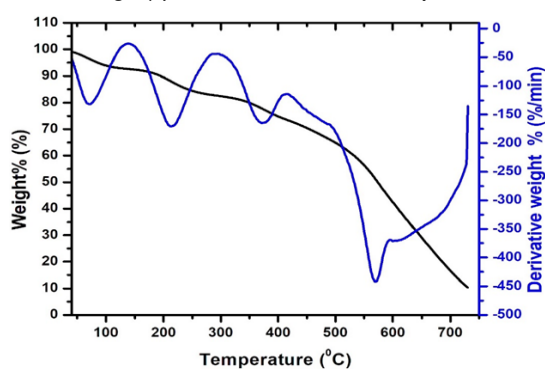


Fig. 2(b). curve of Cu Complex TGA/DTA

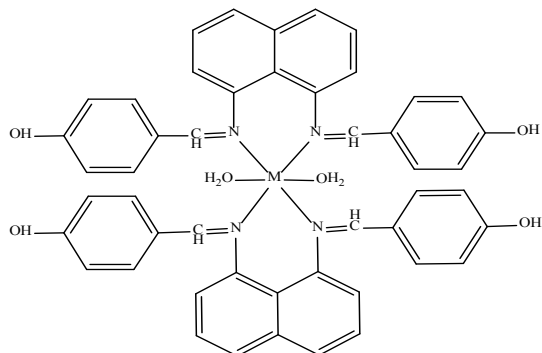


Fig. 3(a). M=Co

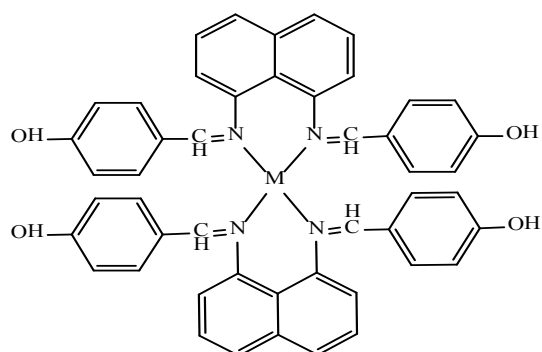


Fig. 3(b). M=Ni, Cu, Zn

Fig. 3. Structure of the complexes

### DFT studies

Density functional theory (DFT) calculation studies were executed using the GAUSSIAN09W program package using B3LYP level with 6-31G(d,p) as the basis set. The optimized structure of the Schiff base was visualized with the help of the GAUSSVIEW 6.0 molecular visualization program.

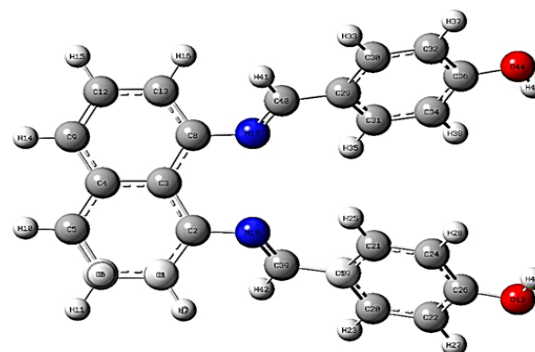


Fig. 4(a). Optimized Structure of NDBDP

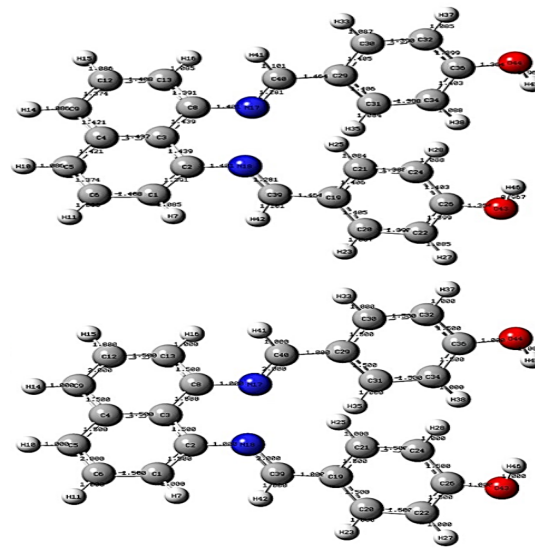


Fig. 4(b). Optimized structure of NDBDP with bond length and bond order

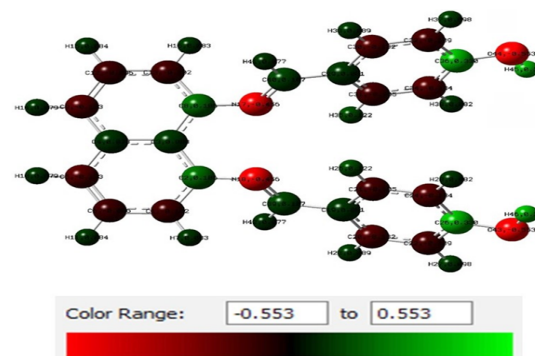


Fig. 4(c). Mulliken charge transfer of NDBDP

### Mulliken charge analysis

The atomic charge distribution of various atoms present in the Schiff base is obtained by Mulliken population analysis. The Mulliken, charges of the Schiff base NDBDP lie between -0.553 and 0.553. The high negative charge is mainly localized on azomethine nitrogen and phenolic OH groups. This confirms the coordination sites of the Schiff base. The different color represents Mulliken charge transfer. Mulliken charge population analysis authenticates the intermolecular charge transfer process.

### Frontier molecular orbitals

The energy gap between HOMO (-0.18608 a.u) and LUMO (-0.05715 a.u) is found to be 0.12893 a.u (3.5084 eV). The HOMO and LUMO energy gap authenticate intramolecular charge transfer interactions. The smallest HOMO–LUMO gap confirms the softness and reactivity of the Schiff base.<sup>34</sup> Energy gap between HOMO–LUMO determines reactivity of the molecule.<sup>35</sup>

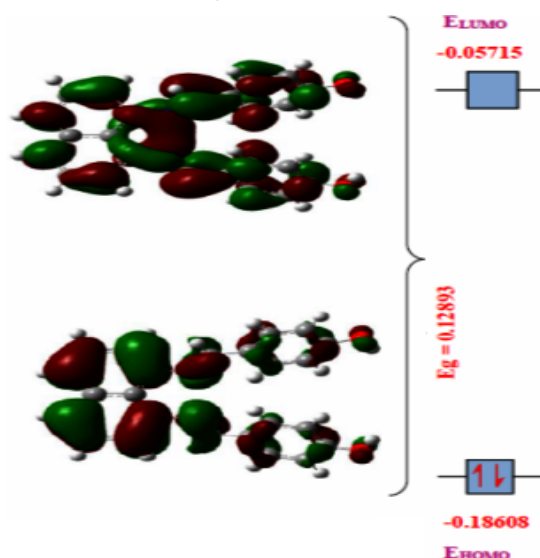


Fig. 5. HOMO-LUMO Energy gap of NDBDP

### Molecular electrostatic potential

The electronegative site (preferred electrophilic attack) in the MEP diagram is indicated in red color. The counter diagrams show the movement of electrons in the Schiff bases. The red region surrounding azomethine group and phenolic group in MEP proves the reactive sites in Schiff base. The contour of the Schiff base was mapped with electrostatic potential, absolute density, HOMO and LUMO.

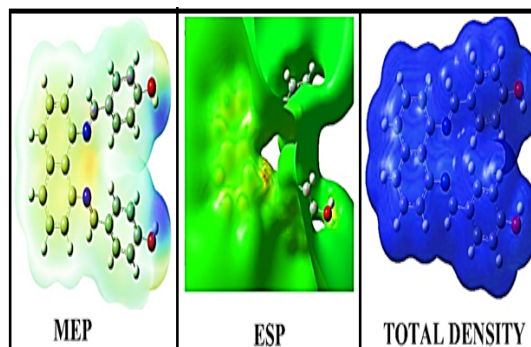


Fig. 6(a). Molecular surface of NDBDP

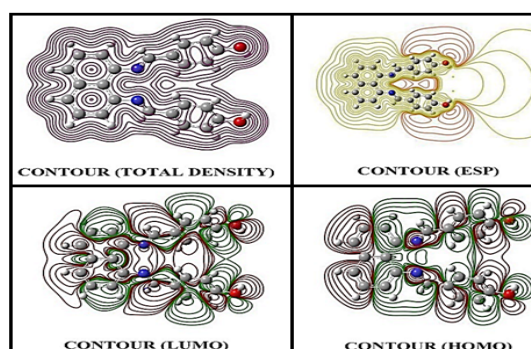


Fig. 6(b). Contour maps of NDBDP

Table 2: Vibrational frequencies of different bonds present in the Schiff base NDBDP DFT/Experimental

Name of the bond	Vibrational Frequency	
	DFT	IR Spectrum (Experimental)
$\nu$ (O-H)	3412	3415
$\nu$ (C=N)	1625	1647
$\nu$ (C=C)	1592	1514
	1392	1444
$\nu$ (C-O)	1248	1242
$\nu$ (C-H)	818	830
	759	761

### Application studies

#### Redox property

The cobalt, copper and zinc complexes, each one exhibit two reduction peaks. The voltammogram of the nickel complex exhibits well denoted redox process. The oxidation and reduction peaks of each complex are given in Table 3. The reduction process is found to be of quasi-reversible process and is all one electron processes<sup>36</sup>. The Cyclic voltammograms are given in Fig. 7(a) to 7(d). The difference between forward and reverse peak potentials observed in all the complexes are all greater than 120 mV, indicating that the redox process is metal centred one electron quasi reversible.<sup>37</sup>

Table 3: Oxidation and Reduction Peaks of Complexes

Name of the Complex	Oxidation Peak (V)	Reduction Peak (V)
(NDBDP) <sub>2</sub> -Co	-1.225 0.0155	-0.9207 -0.0444
(NDBDP) <sub>2</sub> -Ni	0.4142	-0.5697
(NDBDP) <sub>2</sub> -Cu	-1.2083 0.3331	-1.0139 0.8329
(NDBDP) <sub>2</sub> -Zn	-1.3316 -0.1583	1.025 -0.0188

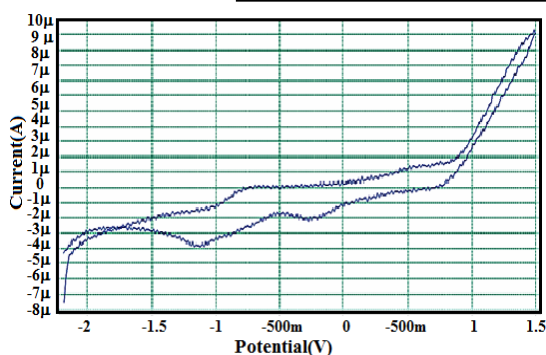


Fig. 7(a). Cyclic voltammogram of Co Complex

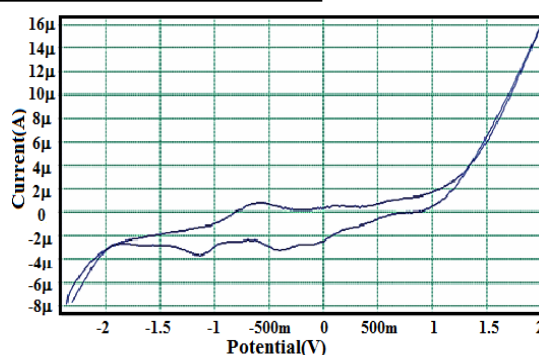


Fig. 7(b). Cyclic voltammogram of Ni Complex

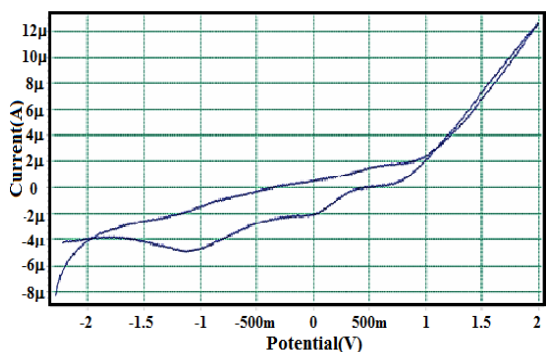


Fig. 7(c). Cyclic voltammogram of Cu Complex

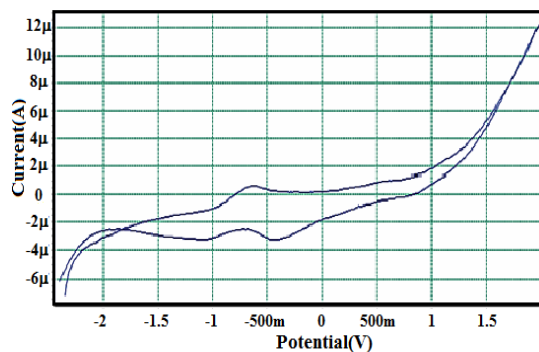


Fig. 7(d). Cyclic voltammogram of Zn Complex

### Antimicrobial activity

The disc diffusion technique is used for scrutinizing the antimicrobial activities of all the compounds. Bacterial pathogens *Staphylococcus aureus* & *Klebsiella pneumonia*, and Fungal pathogens *Aspergillus niger* & *Candida albicans* were taken for the study. Gentamicin and Amphotericin B were used as the positive control. The activities of all the compounds were carried out in a DMSO medium. Considering the bacterial pathogen *Staphylococcus aureus* moderate activity is shown by all the compounds. While with *Klebsiella pneumonia*, the Schiff base ligand shows maximum activity, which is even higher than that of the standard. In the case of a Fungal pathogen namely *Candida albicans*, tremendous activity is observed with both the Schiff base and the Cu(II) complex. (NDBDP)<sub>2</sub>

-Cu complex is found to have 29% higher activity than the standard drug Amphotericin B. The zone of inhibition values and images relating to biological activity are shown in Table 4 & Figure 8.

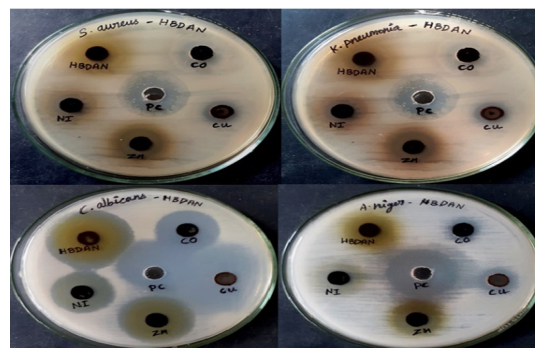


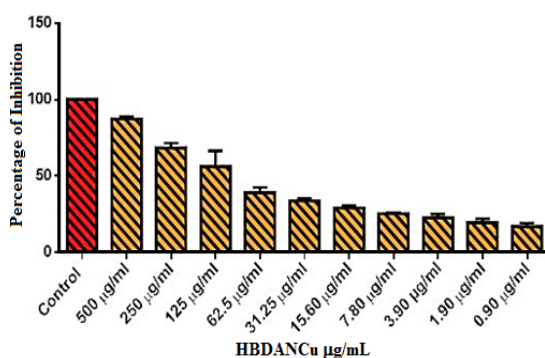
Fig. 8. Antimicrobial activities of the Schiff base and their complexes

**Table 4: Antimicrobial activities of the Schiff base and their complexes**

S.No	Organism	NDBDP	Zone of inhibition (mm)				Control
			[Co(NDBDP) <sub>2</sub> ]	[Ni(NDBDP) <sub>2</sub> ]	[Cu(NDBDP) <sub>2</sub> ]	[Zn(NDBDP) <sub>2</sub> ]	
1	<i>Staphylococcus aureus</i>	14.5	13.5	12.5	12.5	14.5	17.5
2	<i>Klebsiella pneumonia</i>	18.5	12.5	13.5	9.5	14.5	18.25
3	<i>Aspergillus niger</i>	12.5	7.5	11.5	10.25	13.5	16.5
4	<i>Candida albicans</i>	18.5	12.5	14.5	22.5	15.5	17.5

### Minimum Inhibitory Concentration

The outcome of biological analyses unfurl the fact that the copper complex has more excellent activity towards *Candida albicans* than other compounds and organisms studied. Consequently, the copper complex is analysed for MIC studies. The results indicate that the copper complex is sensitive towards *Candida albicans* even at 0.9 µg/mL. Table 5 & Figure 9 show the results.

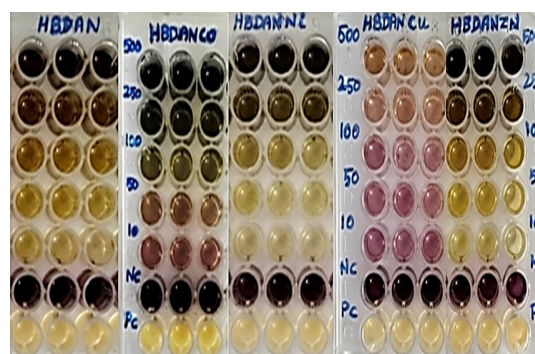
**Fig. 9. MIC of Cu(II) Complex****Table 5: MIC of Copper Complex**

S. No	Tested sample concentration (µg/mL)	Mean value(%)
1	Control	100
2	500	87.34544
3	250	68.45567
4	125	56.06419
5	62.5	39.22652
6	31.25	33.84636
7	15.6	29.22915
8	7.8	25.49329
9	3.9	22.82294
10	1.9	19.41594
11	0.9	16.96922

### Antioxidant activity

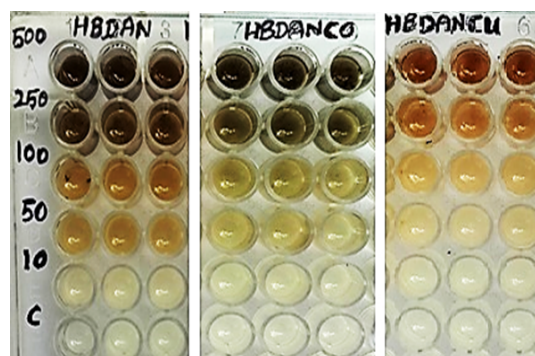
The order of antioxidant activity exhibited by the Schiff base and its complexes was Copper(II) > Cobalt(II) > Schiff base > Zinc(II) > Nickel(II). The potential of the samples to infringement the free radical sequence by

donation of a hydrogen atom<sup>38</sup> clearly explains the order.

**Fig. 10. Anti-oxidant activity of Schiff base and its Complexes**

### Anti-inflammatory activity

The inhibition percentage of albumin denaturation<sup>39</sup> is maximum in the concentration of 500 µg/mL in the case of Schiff base as well as Co & Cu complexes. The order of activity is Schiff base > Co complex > Cu complex.

**Fig. 11. Anti-inflammatory activity of Schiff base, Cobalt & Copper(II) Complexes**

### Anticancer activity

The copper complex is scrutinized for its anticancer activity by applying on MCF-7 cell line through MTT method. Fig. 12 and Table 6 explain the % of cell sustainability in differently concentrated solutions. Comparing the IC<sub>50</sub> value of the complex with that of cisplatin, it is very clear that the copper complex has a moderate cytotoxic effect.



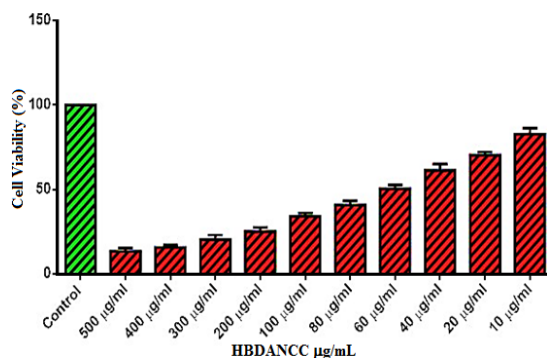


Fig. 12. Anticancer activity of Copper(II) Complex

Table 6: % of Cell Sustainability

Concentration ( $\mu\text{g/mL}$ )	Cell Viability(%)
Control	100
500	13.50522
400	15.77655
300	20.44199
200	25.29159
100	34.19276
80	40.88398
60	50.58318
40	61.32597
20	70.53407
10	82.93432

### CONCLUSION

A new Schiff base NDBDP is synthesized and it is complexed with Co(II), Ni(II), Cu(II) and Zn(II) metals. From spectral & analytical data, the formation of a 1:2 metal-ligand complex is confirmed. The neutral nature of the complexes is proved by their low conductance values. The geometry of the complexes is determined from analytical and spectral studies. Except for the Co(II) complex, which

is proposed octahedral geometry, all other three complexes are proposed square planar geometry. The catalytic application of complexes is revealed by their notable redox property. The Mulliken charge population analysis authenticated the intermolecular charge transfer process. The Schiff base as well as its complexes are established as stupendously bio-potent towards bacterial and fungal pathogens. The Cu(II) complex exhibits greater antioxidant potential than the free Schiff base. The results about anti-inflammatory activity of the Schiff base and its complexes divulge the higher anti-inflammatory activity of Schiff base than its Co(II) and Cu(II) complexes.  $[\text{Cu}(\text{NDBDP})_2]$  exhibits moderate cytotoxic effect over MCF-7 cells.

### ACKNOWLEDGMENT

The authors would like to render their sincere gratitude to the Managing Trustee, the Secretary, the Principal and faculty members of the Chemistry Department, Seethalakshmi Ramaswami College, Tiruchirappalli 620002, Tamil Nadu, India for rendering laboratory facilities and guidance. The authors are also grateful to the Director, SAIF, IIT Madras, Chennai, SAIF (Kochin), Archbishop Casimir Instrumentation Centre (ACIC, St. Joseph's College), Trichy, CARISM (SASTRA Deemed University) and Trichy Research Institute of Biotechnology (P) Ltd, Tiruchirappalli for offering analytical assistance.

### Conflict of interest

The authors declare no competing conflicts of interest to this work.

### REFERENCES

- Fatima, A.; Pereira, C.P.; Raquel Said Dau Gonçalves Olímpio, C.; Germano De Freitas Oliveira, B.; Lopardi Franco, L.; Henrique Corrêa Da Silva, P., *J. Adv. Res.*, **2018**, *13*, 113-126.
- Abdel Rahman, L.H.; Amani, A.; Abdelghani, A.; Al Obaid, A.A.; El Ezz, D.A.; Warad, I.; Shehata, M.R.; Abdalla, E.M.S., *Sci. Rep.*, **2023**, *13*(1), 3199.
- Sikandar, K.; Xiaojing, C.; Albandary, A.; Allehyani, E.S.; Alhumaydhi, F.A.; Ibrahim, M.M.; Ali, S., *J. Environ. Chem. Eng.*, **2021**, *9*(6), (2021) 106381.
- Kargar, H.; Ardakani, R.B.; Torabi, V.; Kashani, M.; Natanzi, Z.C.; Kazemi, Z.; Mirkhani, V.; Sahraei, A.; Tahir, M.N.; Ashfaq, M.; Munawar, K.S., *Polyhedron.*, **2021**, *195*, 114988.
- Dalia, S.A.; Afsan, F.; Hossain, S.; Khan, N.; Zakaria, C.M.; Zahan, K.E.; Ali, M., *Int. J. Chem. Stud.*, **2018**, *6*, 2859-2866.
- Shanmugasundaram, G.; Kumar, K.; Murugesan, S.; Veerasamy, S.; Pounraj, T.; Alagarsamy, M., *J. Mol. Liq.*, **2021**, *325*, 115190.
- Angamaly, A.S.; Jessica, E.P.; Maliyeckal, R.P.K.; Sreedharannair, B.; Puzhavorparambil, V.M., *Bio-org. Chem.*, **2017**, *70*, 67-73.
- Janowska, S.; Khylyuk, D.; Janowski, M.; Kosikowska, U.; Strzyga-Łach, P.; Struga, M.; Wujec, M., *Molecules.*, **2023**, *28*(6), 2718.

9. Chandrasekar, T.; Arunadevi, A.; Raman, N., *J. Coord. Chem.*, **2021**, *74*, 804-822.
10. Ejidike, I.P.; Ajibade, P.A., *Molecules.*, **2015**, *20*, 9788-9802.
11. Sundaravadivel, E.; Reddy, G.; Manoj, D.; Rajendran, S.; Kandaswamy, M.; Janakiraman, M., *Inorganica Chim. Acta.*, **2018**, *482*, 170-178.
12. Kaya, I.; Daban, S.; Senol, D., *Inorganica Chim. Acta.*, **2021**, *515*, 120040.
13. Zoubi, W.A.; Al-Hamdani, A.A.S.; Ahmed, S.D.; Gunko, Y., *J. Phys. Org. Chem.*, **2017**, *31*, e3752.
14. El Sonbati, A.Z.; Mahmoud, W.H.; Mohamed, G.G.; Diab, M.A.; Morgan, S.M.; Abbas, S.Y., *Applied Organometallic Chem.*, **2019**, *33*, e5048.
15. Dongare, P.R.; Gore, A.H.; Ajalkar, B.D., *Inorganica Chim. Acta.*, **2020**, *502*, 119372.
16. Kaur, H.; Lim, S.M.; Ramasamy, K.; Vasudevan, M.; Ali Shah, S.A.; Narasimhan, B., *Arab. J. Chem.*, **2020**, *13*, 377-392.
17. Aggoun, D.; Garcia, M.F.; Daniel, L.; Bouzerafa, B.; Ouennou, Y.; Setifi, F., *Polyhedron.*, **2020**, *187*, 114640.
18. Fonkui, T.Y.; Ikhile, M.I.; Njobeh, P.B.; Ndinteh, D.T., *BMC Chemistry*, **2019**, *13*, 127.
19. Banwell, C.N.; Mccash, M.M. *Fundamentals of Molecular Spectroscopy*, 5<sup>th</sup> ed; Tata McGraw-Hill, New Delhi., **2013**.
20. Ramesh, G.; Daravath, S.; Swathi, M.; Shiva, D., *Chem. Data Collect.*, **2020**, *28*, 100434.
21. Fekri, R.; Salehi, M.; Asadi, A.; Kubicki, M., *Inorganica Chim. Acta.*, **2019**, *484*, 245-254.
22. El-Gammal, O.A.; Mohamed, F.S.; Rezk, G.N.; El-Bindary, A.A., *J. Mol. Liq.*, **2021**, *326*, 115223.
23. Hasan, R.; Hossain, M.A., Salam A., Uddin M.N., *J. Taibah Univ. Sci.*, **2016**, *10*(5), 766-773.
24. El-Sherif, A.A.; Eldebss, T.M.A., *Spectrochim. Acta A.*, **2011**, *9*, 1803-1814.
25. Kumar, D.; Syamal, A.; Sharma, L.K., *Elixir Applied Chemistry.*, **2013**, *54*, 12593-12597.
26. Al-Shaalan, N.H., *Molecules.*, **2011**, *16*, 8629-8645.
27. Gusev, A.N.; Kiskin, M.A.; Braga Kryuk, E.V.; Ova, M.A.; Baryshnikov, G.V.; Karaush-Karmazin, N.N.; Minaeva, V.A.; Minaev, B.F.; Ivaniuk, K.; Stakhira, P.; Agren, H.; Linert, W., *Appl. Electron. Mater.*, **2021**, *3*, 3436-3444.
28. Ucan, S.Y., *Eurasian J. Sci. Eng. Technol.*, **2020**, *1*(1), 35-40.
29. Violet Dhayabaran, V.; Daniel Prakash, T.; Renganathan, R.; Friehs, E.; Bahnemann, D.W., *J. Fluoresc.*, **2017**, *27*, 135-150.
30. Bassett, J.; Denney, R.C.; Jeffery, G.H.; Mendham, J. *Vogel's Textbook of Quantitative Inorganic Analysis including Elementary Instrumental Analysis.*, Longman Group Limited., **1978**, *311*, 322.
31. Hammam, A.M.; El-Gahami, M.A.; Khafagi, Z.A.; Al-Salimi, M.S.; Ibrahim, S.A., *J. Mater. Environ. Sci.*, **2015**, *6*(6), 1596-1605.
32. Chetana, P.R.; Siddaramaiah, X.; Ramappa, P.G., *Thermochim. Acta.*, **2005**, *425*, 13-21.
33. Amala, S.; Santhi, S.; Subashini, S., *Chemistry Select.*, **2018**, *3*, 7378-7384.
34. Messasma, Z.; Ourari, A.; Mahdadi, R.; Houchi, S.; Aggoun, D.; Kherbache, A.; Bentouhami, E., *J. Mol. Struct.*, **2018**, *1171*, 672-681.
35. Alam, M.S.; Lee, D.U., *Spectrochim Acta A Mol Biomol Spectrosc.*, **2015**, *145*, 563-574.
36. Aggoun, D.; Garcia, M.F.; Lopez, D.; Bouzerafa, B.; Ouennoughi, Y.; Setifi, F.; Ourari, A., *Polyhedron.*, **2020**, *187*, 114640.
37. Raman, N.; Raja, J.D.; Sakthivel, A., *J. Chem. Sci.*, **2007**, *119*(4), 303-310.
38. Hernandez, J.A.; Jimenez, A.; Mullineaux, P.; Sevilla, F., *Plant Cell Environ.*, **2002**, *23*, 853-862.
39. Sakat, S.; Juvekar, A.R.; Gambhire, M.N., *Int J Pharm Pharm Sci.*, **2010**, *2*(1), 146-156.